IDENTIFICATION OF MAGNETIC BEARING SYSTEMS

Conrad Gähler

International Center for Magnetic Bearings, ETH Zurich, Switzerland

Raoul Herzog

Mecos Traxler AG, Winterthur, Switzerland

ABSTRACT

System identification allows fast and accurate modelling of magnetic bearing systems. It makes static measurement of bearing characteristics and modal analysis of flexible rotors obsolete. This eliminates the need for the related expensive measurement equipment, and results in a substantial reduction in the time required for commissioning. Moreover, the achieved control performance can be improved.

Identification of magnetic bearings must be tailored to the controller. Strategies for this are proposed. Experimental results for various set-ups are presented.

1. INTRODUCTION

Motivation

A parametric dynamic model of the magnetic bearing system is required for the controller design. If the plant dynamics are not exactly known, the controller has to be robust with respect to this plant uncertainty, or else it may fail to meet the performance requirements with the real plant. However, it is well known [1] that higher controller performance can be achieved if less robustness is required - in other words, if the plant is more exactly known.

Presently, the dynamic plant model is established based upon theoretical knowledge. For instance, the bearing parameters k_i and k_s are computed from geometry, winding number, nominal air gap and bias current. The dynamics of flexible rotors are computed using FE modelling. This theoretical model is often adjusted by static measurement of the bearing parameters and by a modal analysis of the rotor [2]. Both measurements are quite cumbersome. Moreover, many phenomena cannot be assessed with this method. Examples for this are sensor and amplifier dynamics, eddy current and hysteresis effects. Another example is the reduction of the rotor's natural frequencies with rotating speed, as the shrink fits are loosened under the influence of centrifugal forces.

Goals

Identification of the plant dynamics between controller output and controller input gives an accurate model of the complete plant, incorporating all these effects. Thus, it allows

- to circumvent time consuming and expensive modal analysis and static force measurements at initial set-up
- to improve the accuracy of the plant input-output model
- to achieve better controller performance
- to give a better insight into the physical behaviour of the AMB system

2. MEASUREMENT TOOLS

Today's AMB systems are often controlled by means of a digital controller board. This is usually connected to a host PC for development and controller design. For our controller boards, we have designed a comfortable inter-

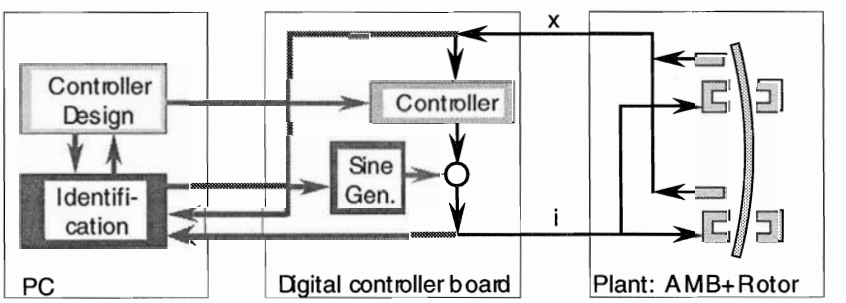

FIGURE 1: Measurement set-up for identification of AMB systems. Different signals can be chosen to be plant's inputs and outputs.

face from the standard mathematics package MATLAB [3]. This allows to read and write all variables in the program of the digital controller. The sine wave generator used for excitation of the plant is programmed on the controller processor. Data acquisition (*i.e.,* recording the time history of certain signals) is done with the controller board as well. These data are transferred to the PC for computation of transfer function, identification, and controller design. Excitation, data acquisition and data transfer can be controlled from within MATLAB. Thus, the measurements needed for identification can be done without any additional hardware. The whole set-up is shown in figure 1.

The proposed algorithms are based on frequency response function (FRF) measurement. Sine wave excitation yields an excellent signal-to-noise ratio in the data acquisition. Based on these FRF data, a parametric model (rational transfer function) is constructed.

3. LEAST SQUARES ALGORITHMS

In this section, two methods for modelling the open-loop behaviour of an AMB plant are presented. In section 4 we will show that it is rather the closed-loop behaviour that must be approximated by identification. However, the methods of section 4 use the same framework as those in section 3.

For the sake of simplicity, we treat the SISO case only in this paper. The results, however, can be applied to MIMO problems as well. Furthermore, we do not go into details about the distinctions between continuous and time-discrete identification.

3.1. Preliminaries

Let denote

N the number of frequency points at which the plant transfer function has been measured

ω_k with $k = 1 \,..\, N$
the measurement frequencies

$\tilde{P}(s = j\omega_k)$
the measured plant transfer function at frequency ω_k

$$\hat{P}(s) = \frac{B(s)}{A(s)} \tag{3.1.1}$$

the identified, parametric transfer function in the usual form of a rational polynomial fraction

$B(s) = b_m s^m + b_{m-1} s^{m-1} + \ldots + b_0$

$A(s) = s^n + a_{n-1} s^{n-1} + \ldots + a_0$
the nominator and denominator polynomials of $\hat{P}$

m, n the degrees of the nominator and denominator polynomials. We assume that we know m and n *a priori*. This assumption is reasonable in the case of AMB systems.

$\vartheta = [b_m \;\; \ldots \;\; b_0 \;\vdots\; a_{n-1} \;\; \ldots \;\; a_0]'$
the vector of the coefficients of $B(s)$ and $A(s)$.

Identification has the goal to find the coefficients a_i, b_i of the polynomials A(s), B(s) such that $\tilde{P}$ is approximated by $\hat{P}$ in some sense. To be more specific, we define the error

$$\boldsymbol{e} = [e_1 \ldots e_N]' = \boldsymbol{e}(\tilde{P}, \hat{P}) \tag{3.1.2}$$

This error can be defined in different ways, as we will see below. With least squares algorithms, the identification criterion that has to be minimised is defined by the 2-norm of $\boldsymbol{e}$: We look for

$$\vartheta^* = \arg\min_{\vartheta}(\|\boldsymbol{e}\|_2) = \arg\min_{\vartheta} \sqrt{\sum_{k=1}^{N} e_k{}^2} \tag{3.1.3}$$

3.2. Minimising the absolute model error

Minimising the absolute error means solving (3.1.3) with

$$e_k = \tilde{P}(j\omega_k) - \frac{B(j\omega_k)}{A(j\omega_k)} \tag{3.2.1}$$

This involves a non-linear optimisation. Multiplying the right hand side of (3.2.1) with $A(s)$, *i.e.,* choosing

$$e_k = A(j\omega_k) \cdot \tilde{P}(j\omega_k) - B(j\omega_k) \tag{3.2.2}$$

instead makes the problem (3.1.3) linear in the parameters, but does not yield the correct solution of the original problem: A(s) is a weighting to the problem (3.1.3). The fit is improved at frequencies where $A(j\omega)$ is large, and deteriorated where $A(j\omega)$ is small.

Sanathanan and Koerner [4] have proposed an iterative

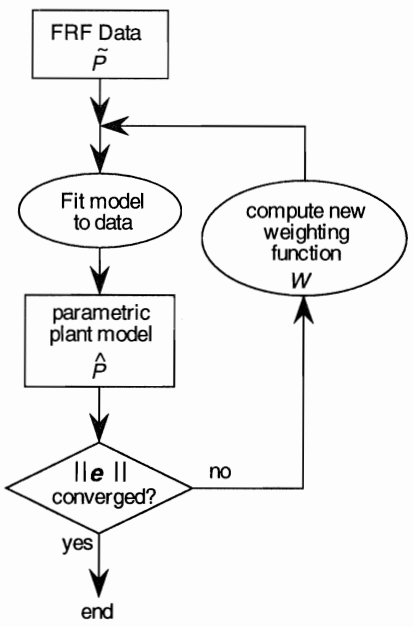

FIGURE 2: Iterative identification scheme

algorithm to obviate this shortcoming (*cf* figurwe 2). They suggest to use

$$e_{k,i} = \left(A_i(j\omega_k)\cdot\tilde{P}(j\omega_k) - B_i(j\omega_k)\right)\cdot W_i(j\omega_k) \quad (3.2.3)$$

Thereby, the weight W_i used for the i-th iteration is chosen as

$$W_i(j\omega_k) = \frac{1}{A_{i-1}(j\omega_k)} \quad . \quad (3.2.4)$$

For the first iteration, W_1 can be chosen unity for all frequencies.
This algorithm removes undesired weightings whilst preserving linearity in the parameters for (3.1.3). The algorithm converged always in our applications. However, convergence cannot be proved. The result can be refined using numerical optimisation [5].

3.3. Minimising the relative model error

Magnetic bearing systems have a roll-off of 40 dB per decade with current control, and even 60 dB per decade with voltage control [6,7]. Minimising the absolute error therefore yields poor results at high frequencies. Minimising the relative error gives better approximations. This means solving (3.1.3) with

$$e_k = \frac{\tilde{P}(j\omega_k) - B(j\omega_k)/A(j\omega_k)}{\tilde{P}(j\omega_k)} \quad (3.3.1)$$

The method explained above can easily be applied to this error criterion by choosing

$$W_i(j\omega_k) = \frac{1}{A_{i-1}(j\omega_k)\cdot\tilde{P}(j\omega_k)} \quad (3.3.2)$$

3.4. Identification of k_i and k_s using *a priori* - knowledge on the rotor dynamics

If the dynamic behaviour $P_R(s)$of the rotor is known (*e.g.*, from a modal analysis), it is possible to compute k_i and k_s from FRF measurement and this a priori knowledge [8]. We then know to be

$$\hat{P}(s) = \frac{k_i}{1 - k_s\cdot P_R(s)} \quad (cf.\ \text{figure 3}).$$

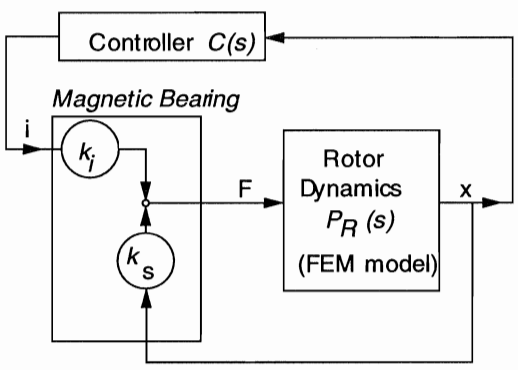

FIGURE 3: Identification of k_i and k_s with known rotor dynamic model $P_R(s)$

Measurements at a few low frequencies, along with knowledge of the rigid body dynamics of the rotor, are sufficient to determine k_i and k_s.

3.5. Experimental results

Minimisation of the relative model error (section 3.3) without using *a priori* knowledge has been applied to an AMB test stand with a flexible rotor. The MIMO AMB plant has been separated into two SISO plants:

$$\begin{bmatrix} P_1 & P_2 \end{bmatrix} = \begin{bmatrix} \frac{x_a + x_b}{i_a + i_b} & \frac{x_a - x_b}{i_a - i_b} \end{bmatrix},$$

where index a and b refer to the two bearings. This separation could be done because the rotor was symmetric. The results have been obtained for the plant P_1 which describes the translation mode and the first, third, ... flexible modes.
The result is shown in figure 4. The poles of the transfer function are estimated well already at the first iteration step, while the zeros must be improved in the second step using (3.3.2). A dead time was introduced to account mainly for amplifier dynamics. The plant order of 6 (three modes) was determined *a priori*.
A comparison of measured FRF and the FRF of the identified model shows that the dynamics of the rotor as well as the bearing parameters can be identified accurately. We can thus say that measurement of the bearing characteristics as well as modal analysis have become obsolete thanks to identification.

The method described in section 3.4 has been applied to the same plant. The rotor model was taken from FE calculations and included the translation mode and the first flexural mode. The fit achieved about the same precision as the one in Figure 4.

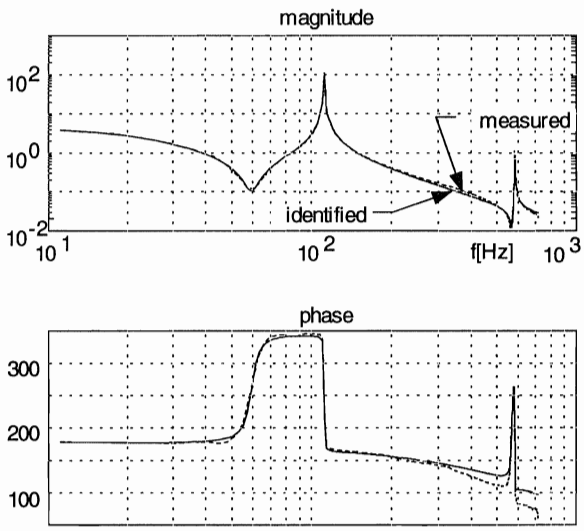

FIGURE 4: Identification of an AMB system with flexible rotor without *a priori* knowledge. Current control.

4. IDENTIFICATION FOR CONTROL

4.1. Concept and algorithm

In section 3, we have presented a method for minimising the absolute or the relative model error. Absolute and relative model errors are "open-loop properties" of the model. However, a model's capability of reproducing well the plant's open loop characteristics does not necessarily imply its suitability for controller design. This follows from basic results in robust control theory.

Let denote

$\hat{P}(s)$ the nominal plant (parametric model obtained from identification)

$\tilde{P}(s)$ the true plant

$P(s)$ some arbitrary plant

C a controller that stabilises $\hat{P}$

$\Delta = \tilde{P} - \hat{P}$

the additive model error

$$\hat{S}(j\omega) = \frac{1}{1 + \hat{P}(j\omega) \cdot C(j\omega)}$$

the *designed sensitivity function*

$$\tilde{S}(j\omega) = \frac{1}{1 + \tilde{P}(j\omega) \cdot C(j\omega)}$$

the *achieved sensitivity function*

Robust stability. $C(s)$ will stabilise all plants $P(s)$ for which the following inequality holds *(small gain condition)*:

$$\left|P(j\omega) - \hat{P}(j\omega)\right| < \left|\frac{1}{C(j\omega) \cdot \hat{S}(j\omega)}\right|, \quad \forall\omega \qquad 1)$$

Conversely, for arbitrarily small $\delta(j\omega)$ there are plants $P(s)$ with

$$\left|P(j\omega) - \hat{P}(j\omega)\right| < \left|\frac{1}{C(j\omega) \cdot \hat{S}(j\omega)}\right| + \delta(j\omega), \quad \forall\omega$$

which are not stabilised by C. Therefore, an arbitrarily small model error Δ (at a frequency where $\left|C \cdot \hat{S}\right|$ is large) can lead to instability.

In other words: The controller determines to a large extent how large a model error Δ can be accepted at a certain frequency. This means that not only the controller design depends on the model, but also the modelling depends on the controller. This gives rise to an iterative scheme, as proposed by [5,9]: Modelling and identification are no longer be considered as two independent problems, but rather as one joint problem. Inserting figure 3 into this scheme, we like to state it as shown in figure 5. (This iterative scheme must be kept in mind also if different identification methods are used!)

There are different strategies for identification in view of this fact. We just mention two of them.

Sensitivity function as weighting function. We certainly need an accurate model where the sensitivity function is large. Therefore we can minimise the (absolute or relative) error weighted by the sensitivity function,

$$e = \left\| \left(\tilde{P} - \hat{P}\right) \cdot S \right\| \text{ or } e = \left\| \frac{\tilde{P} - \hat{P}}{\tilde{P}} \cdot S \right\|, \qquad (4.1.1a,b)$$

by choosing

$$W_i = \frac{S_{i-1}}{A_{i-1}} \text{ or } W_i = \frac{S_{i-1}}{A_{i-1} \cdot \tilde{P}} \qquad (4.1.2a,b)$$

S can thereby be the designed or the achieved sensitivity function.

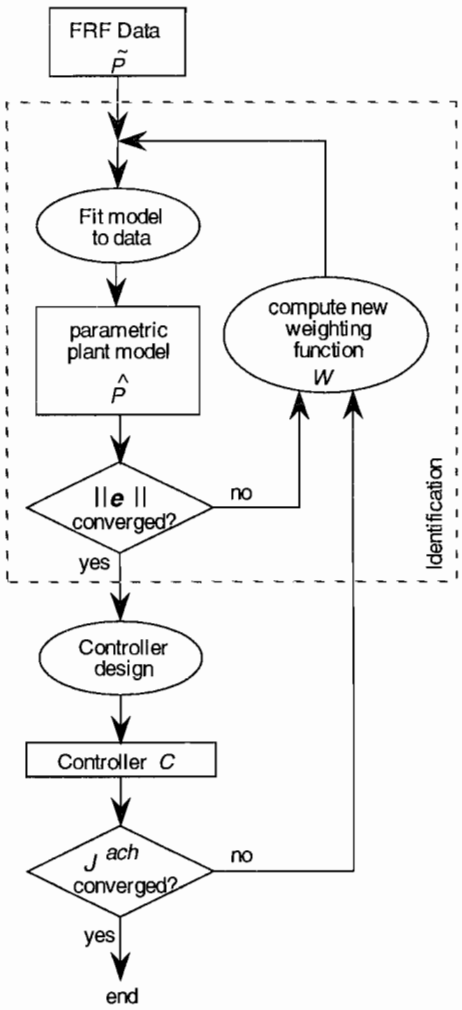

FIGURE 5: Iterative scheme: Joint design of identification and control

1) To be exact, this holds if P and $\hat{P}$ have the same number of unstable zeros.

Achieved performance. The objective of the controller design for AMB systems is disturbance attenuation: The effect of disturbance inputs (noise, disturbance forces) on system outputs (displacements, coil currents, and coil voltages) have to be small. The related closed-loop transfer functions (from disturbance inputs to system outputs) must be kept small in some sense. As they all contain the sensitivity function S as a common factor, it is a valid approach to define the controller performance J by some norm of the weighted sensitivity function [1,7]:

$$J\left(\tilde{P},C\right)=\left\|W_p\cdot S\left(\tilde{P},C\right)\right\|_\infty, \text{ or} \qquad (4.1.3)$$

$$J\left(\tilde{P},C\right)=\left\|W_p\cdot S\left(\tilde{P},C\right)\right\|_2 \qquad 2) \ (4.1.4)$$

The weighting W_p is thereby a design parameter of the controller. A reasonable goal for the identification is then to create a plant model $\tilde{P}$ such that the *achieved performance,*

$$J^{ach}=J\left(\tilde{P},C\right)$$

is as close as possible to the *designed performance,*

$$J^{des}=J\left(\hat{P},C\right)$$

This can be achieved by choosing the weighted error in the sensitivity function as an identification criterion:

$$e_k=W_p(j\omega_k)\cdot\left(\tilde{S}(j\omega_k)-\hat{S}(j\omega_k)\right) \qquad (4.1.5)$$

which is equal to

$$e_k=W_p\,C\,\tilde{S}\,\hat{S}\,\frac{1}{A}\cdot\left(\tilde{P}\cdot A-B\right) \qquad (4.1.6)$$

From this it follows that we can apply (3.2.3, 3.1.3) with

$$W_i=W_p\,C\,\tilde{S}\,\hat{S}_{i-1}\,\frac{1}{A_{i-1}} \qquad (4.1.7)$$

4.2. Experimental results with a self-sensing bearing system

Plant description. With the self-sensing bearing, the coil currents are used as measurements while the coil voltages are used as command signals [6,7]. The advantage of this configuration lies in the fact that no position sensor is needed.

For a system with two opposing coils and one degree of freedom, the linearised system equations are

$$\frac{d}{dt}\begin{bmatrix}x\\ \dot{x}\\ i\end{bmatrix}=\begin{bmatrix}0 & 1 & 0\\ 2k_i/m & 0 & 2k_s/m\\ 0 & -2k_i/L & -R/L\end{bmatrix}\cdot\begin{bmatrix}x\\ \dot{x}\\ i\end{bmatrix}+\begin{bmatrix}0\\ 0\\ 1/L\end{bmatrix}\cdot u \qquad (4.2.1)$$

Thereby, L denotes the total inductance (including stray inductance), and R the copper resistance of the coils. The nominal air gap is 3.5 mm.

It is important to note that the system is both non-minimum phase and unstable and therefore really difficult to control. In fact, the unstable pole and the unstable zero are even quite close to each other in our experimental system. The poles and zeros (as found by identification) are at

$p_{1,2}$ = - 48.4±17.1 rad/s, p_3 = + 60.0 rad/s
z_1 = - 91.7 rad/s, z_2 = + 76.15 rad/s

Experiment. The joint identification/controller design scheme, as shown in figure 5, has been applied to this plant. The controller was thereby designed by the LQG method. The steps of the iteration have been chosen in the following way:

- Iteration 1, Start-up: Identification of the plant by minimising the relative error of the transfer function; controller design based on the resulting model
- Iterations 2 .. 22: Identification using (4.1.2a) or (4.1.7), with W_p = unity. New controllers based on the new identification results were designed at iterations 1, 2, 4, 7, 10, 13, 16, 19, and 22.

Results.

- In the first identification step, the plant can be identified with a relative model error smaller than 10% for all frequencies. All the same, the controller C_1 that has been designed on the basis of the model from step 1 does not stabilise $\tilde{P}$. This can be predicted by computing the Nyquist curve $C_1\tilde{P}$.
- Between the controller design steps, the identification procedure converges. This can be seen from the flat parts in the graph of the error criterion, figure 6.
- Refined modelling allows for an improved controller performance (4.1.4) at each controller design step. This is shown in figure 7.
- The resulting controller has been implemented and tested with the real plant. Although the sensitivity function is still very high (figure 8), the designed controller stabilises the plant well without further tuning. Figure 9 shows the response of the AMB system with the designed controller to a force impulse.

5. CONCLUSIONS

Methods of system identification have been successfully applied to various AMB systems. Results have been presented for current controlled AMBs with a flexible rotor, and for a self-sensing AMB system. Modelling the open-loop characteristics is sufficient in some cases. In general, however, an iterative scheme of identification

2) Note that with all controller design methods, it is a primary goal to keep the sensitivity function small: This goal is explicitely formulated in methods such as H_∞ or LQG/LTR. With pole placement, it has to be achieved by choosing appropriate pole locations; with LQG without loop transfer recovery by selecting appropriate weighting matrices.

and controller design, as outlined in this paper, yields better results.

On the example of the self-sensing bearing we have demonstrated that a controller design for a "difficult" plant with a high resulting sensitivity function worked without further tuning. Both the designed and the achieved performance could be improved thanks to appropriate modelling. Both controller design and identification can still be improved. Further, the proposed scheme will have to be applied to other AMB configurations.

REFERENCES

1. Morari, M., Zafiriou, E.: Robust Process Control. Prentice Hall, 1989
2. Schweitzer, G., Traxler, A., Bleuler, H.: Active Magnetic Bearings. Verlag der Fachvereine, Zurich, Switzerland, 1994
3. Herzog, R., Siegwart, R.: High Performance Data Acquisition, Identification, and Monitoring for Active Magnetic Bearings. 2nd Int. Symp. on Magnetic Suspension Technology, NASA, Seattle/USA, Aug. 11-13, 1993
4. Sanathanan, C. K., Koerner, J.: Transfer Function Synthesis as a Ratio of Two Complex Polynomials. IEEE Trans. Automatic Control, Vol. 8, 1963
5. Schrama, R.: Approximate Identification and Controller Design. PhD Thesis, Delft University of Technology, 1992
6. Dieter Vischer: Sensorlose und spannungsgesteuerte Magnetlager. PhD Thesis Nr. 8665, Swiss Federal Institute of Technology, Zurich, 1988
7. R. Siegwart et al.: Control Concepts for Active Magnetic Bearings. Int. Symp. on Magnetic Suspension Technology, NASA Langley Research Center, Hampton, VA, August 19-23, 1991
8. Herzog, R., Gähler, C.: Modelling and Identification of Flexible Rotors in Magnetic Bearings. MATHMOD, Vienna, February 2-4, 1994
9. Gevers, M.: Towards a joint design of identification and control? Technical report, Dept. Automatic Control, University of Louvain, Belgium, 1993

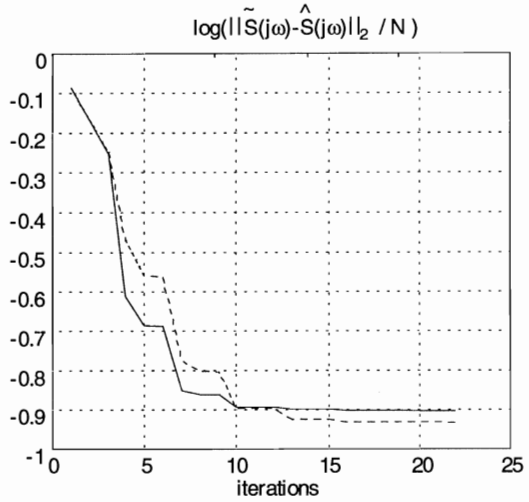

FIGURE 6: Mismatch of the sensitivity functions as a function of the number of iterations. Weightings from equations (4.1.2a) (solid), and (4.1.7) (dashed).

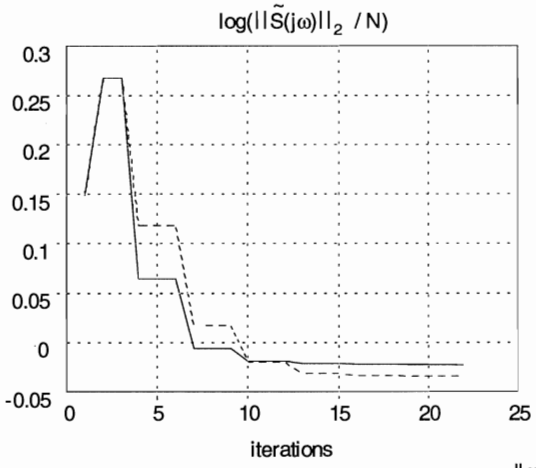

FIGURE 7: Achieved controller performance $\|\tilde{S}\|_2$ as a function of the number of iterations.

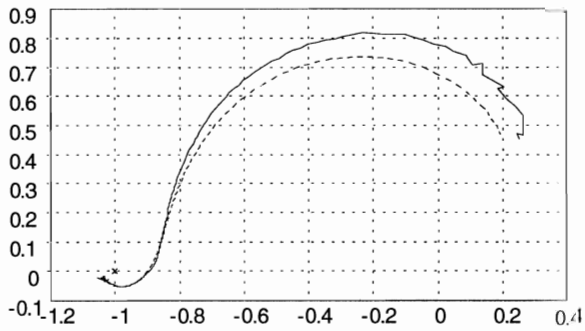

FIGURE 8: Nyquist plot after iteration 22. Solid: $C\tilde{P}$; dashed: $C\hat{P}$. Identification with weighting from (4.1.7). Frequency range is 10 .. 2000 rad/sec.

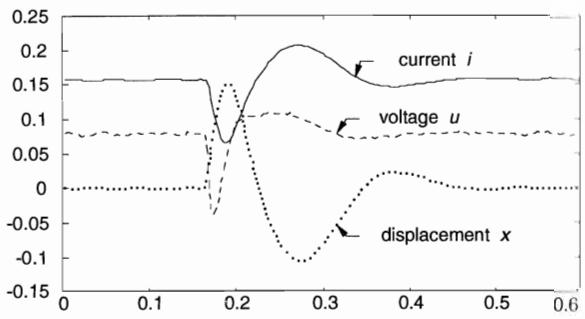

FIGURE 9: Measured response to a force impulse after iteration 22. All quantities are scaled with respect to their maximal values (nominal air gap, maximum current and voltage).